Substituent Effects on the Excited-State Properties of Platinum *meso*-Tetraphenylporphyrins

Beauford W. Atwater[1]

A study has been undertaken to examine the effect of peripheral substitution on the photophysics of platinum tetraarylporphyrins. The aim of the study was to provide better dyes for oxygen sensing. Substitution of electron rich aryl groups results in red shifts for both the absorption and emission spectra. These observations are explained using simple molecular orbital theory. The lifetime of the excited singlet state for platinum tetraphenylporphyrin is calculated to be shorter than 0.7 psec. The radiative rate constants are on the order of 10^3 sec^{-1} while nonradiative rate constants are on the order of 10^4 sec^{-1}. The model used is sufficiently flexible to be applied to all Pt and Pd porphyrins.

INTRODUCTION

Platinum and palladium porphyrins show intense room-temperature phophorescence. They have high triplet-state yields and short triplet-state lifetimes. An interesting technical application of these properties is the use of such porphyrins as oxygen probes. Indeed, platinum and palladium porphyrins have been used as probes for imaging the oxygen distribution in tissue [1–3], in thin films [4], and along aerodynamic surfaces [5]. Platinum porphyrins have a triplet state lifetime shorter by an order of magnitude compared to analogous Pd porphyrins while having similar emission yields. Consequently, Pt porphyrins can be used in applications where a higher concentration of oxygen must be measured.

An important application for oxygen probes is in remote sensing of the arterial blood gases using optical fibers [6,7]. Platinum porphyrins are ideal candidates for such probes since a fast oxygen response and a wide dynamic range of oxygen concentration are critical [8].

Several factors combine to make the specific choice of platinum porphyrin important. The optical fibers are small and thus the amount of emission which can be coupled into a fiber is limited. To maximize this emission, it is important to match simultaneously the absorption spectrum of the porphyrin to the excitation source and the emission spectrum to the detector. Also important is the triplet-state lifetime of the porphyrin sensor; shorter triplet-state lifetimes lead to less emission quenching at high concentrations of oxygen and hence more signal to the detector. A study was undertaken to determine the factors which affect the absorption and emission spectra and phosphorescent lifetimes of Pt *meso*-tetraarylporphyrins. It was hoped that the results of this study could be used broadly to determine the structures of any Pd or Pt porphyrin for use in a particular application involving oxygen sensing. The *meso*-tetraarylporphyrins were chosen so that Hammett substituent constants could be used and that inductive and resonance effects could be isolated.

A model was needed that could be used to correlate electronic substituent effects with the energies of the porphyrin visible bands. The effect of peripheral substitution on the state transitions in porphyrins has been dealt with both qualitatively and quantitatively using

[1] The BOC Group Technical Center, 100 Mountain Avenue, Murray Hill, New Jersey 07974.

Gouterman's four-orbital model. From the energies and intensities of the visible bands, this model provides the energies and the transition dipoles for the two singly excited one-electron configurations and the degree of configuration interaction between them. Gouterman's four-orbital model was used to determine these properties of the frontier molecular orbitals responsible for the visible bands for a series of Pt porphyrins. In the present study, the effects of peripheral substitution on these molecular orbitals were examined. The triplet-state lifetimes and emission yields were also measured for this series.

MATERIALS AND METHODS

The following abbreviations are used for the porphyrins: Pt *meso*-tetraphenylporphyrin, Pt TPP; Pt *meso*-tetra(*p*-cyanophenyl)porphyrin, Pt PCN; Pt *meso*-tetra(*p*-bromophenyl)porphyrin, Pt PBr; Pt *meso*-tetra(*p*-hydroxyphenyl)porphyrin, Pt POH; Pt *meso*-tetra(*p*-trifluoromethylphenyl)porphyrin, Pt CF3; Pt *meso*-tetra(*p*-aminophenyl)porphyrin, Pt PNH2; Pt *meso*-tetra(*p*-methoxyphenyl)porphyrin, Pt POMe; Pt *meso*-tetra(*p*-carbomethoxyphenyl)porphyrin, Pt PCM; Pt *meso*-tetra(pentafluorophenyl)porphyrin, Pt PF5; and Zn *meso*-tetraphenylporphyrin, Zn TPP.

The Pt porphyrins were either synthesized or obtained from Porphyrin Products. The procedures of Adler *et al.* [9] (Pt PCN, Pt TPP, Pt PBr, Pt POH, Pt PCF3) and Lindsey *et al.* [10] (Pt CF3, Pt PCN, Pt PCM) were used to synthesize the porphyrins. The metallation was accomplished by heating the porphyrin with $PtCl_2$ in benzonitrile at reflux [11]. The porphyrins were purified by column chromatography (Florisil, methylene chloride/ethyl acetate) and recrystallization (methylene chloride/ethanol). Those from Porphyrin Products (Pt POH, Pt PNH2, Pt POMe, Pt PCF3, Pt PCM, and Pt PF5) were used as received. Zn TPP was obtained from Aldrich and used without further purification. *N,N*-Dimethylaniline was obtained from Aldrich and purified by distillation.

Absorption spectra were measured on a Perkin–Elmer Lambda 6 spectrophotometer using 1.0-nm slits. The spectra were measured at room temperature in tetrahydrofuran in 1-cm cells and at 77 K in 3-mm quartz ESR tubes. Effects due to aggregation were checked by diluting the samples by 10 and using 10-cm-pathlength cells. No changes in the absorption spectra were noted. Emission spectra were measured on an ISS GREG 200 fluorimeter. Samples of the platinum porphyrins were rigorously degassed with several freeze–pump–thaw cycles on a vacuum system to less than 1×10^{-6} Torr. The samples were excited with the 514.5-nm line from a

Cyonics Model 2202 Argon ion laser. The emission was measured through 4-nm-bandpass slits on an ISA H-10 monochromator and focused on a Hamamatsu R928 photomultiplier tube. The spectra were corrected for instrument response. Emission yield determinations were made with *meso*-tetraphenylporphyrin in benzene as a standard, $\Phi = 0.11$ [12], and were corrected for the difference in the index of refraction. Lifetime measurements were made with the GREG200 fluorimeter. The excitation, 514.5 nm, was modulated sinusoidally with an Intraaction AOM-80 acousto-optic crystal driven by a Hewlett–Packard Model 3325a frequency synthesizer. The photomultipliers were modulated with a Hewlett–Packard Model 3325a frequency synthesizer amplified by either an ITECO 30W or an ENI Model 6031 RF amplifier. The standard was tetraphenylporphyrin in benzene, $t = 0.017$ μs [13]. The frequencies used were sufficient to keep the modulation ratio between 0.1 and 0.9. The average phase and modulation values at several frequencies were fit using a nonlinear least-squares analysis to a long-lived exponential decay and scattered light.

RESULTS

Visible Absorption Spectra

Visible absorption spectra of metalloporphyrins consist of two sets of bands: one in the 500- to 600-nm region and one in the near-ultraviolet. The green bands result from transitions between the ground state and the first excited state, Q(0,0) and Q(1,0), which have zero and one quantum of vibrational energy each, respectively. The more intense B bands are in the blue region and arise from transitions from the ground state to the second excited state. Both sets of bands are π,π^* in origin [14]. The absorption spectra of Pt TPP, Pt PNH2, Pt POH, and Pt PCF3 are shown in Fig. 1. The absorption maxima and extinction coefficients for the substituted platinum porphyrins are listed in Table I. Substitution of electron releasing groups at the *para* position of the tetraphenylporphyrins results in a bathochromic shift of the B band. Strong electron withdrawing substituents shift the B band energy to the blue. The Q band energies are affected only slightly by substitution at the *para* position. Electron releasing substituents lower and broaden the absorption intensities of the Q and B bands and lead to a decrease in the ratio of the Q-to-B band intensities.

Band energies and intensities for the visible absorption spectra can be explained adequately by examining the frontier molecular orbitals involved [15–17]. In metalloporphyrins with d_{4h} symmetry, the lowest-en-
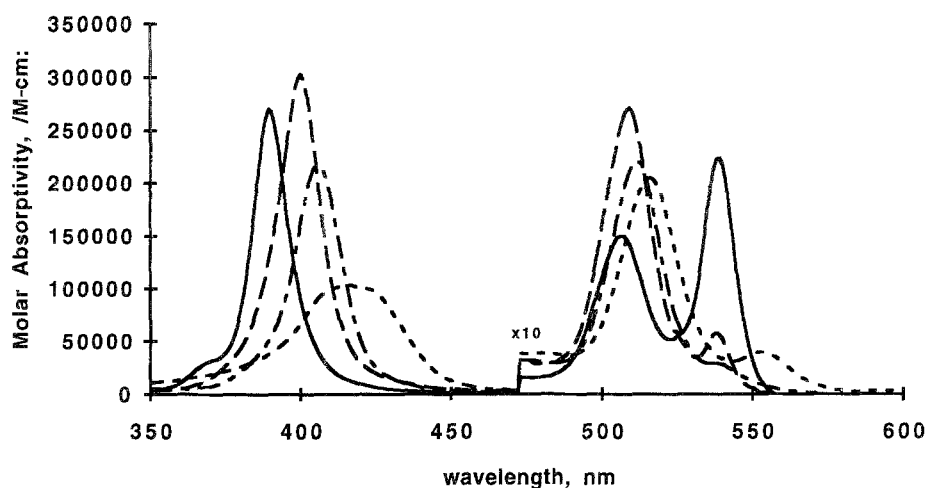
Fig. 1. Absorption spectra for Pt TPP (————), Pt PNH2 (-----), Pt POH (—·—), and Pt PF5 (————).

Table I. Absorption Maxima, Peak Widths, Molar Extinction Coefficients, and Oscillator Strengths for B and Q Bands for Substituted Pt *meso*-Tetraarylporphyrins

	B, max (nm)	fwhm (cm^{-1})	ϵ $(10^5\ M^{-1}\ cm^{-1})$	$f(B)$ (10^8)	Q, max (nm)	fwhm (cm^{-1})	ϵ $(10^3\ M^{-1}\ cm^{-1})$	$f(Q)$ (10^6)
Pt PNH2	418	1834	1.06	1.9	552	688	3.06	2.10
Pt POH	406	1205	2.40	2.9	538	518	2.88	1.49
Pt TPP	399	1005	3.01	3.0	537	416	5.86	2.44
Pt TBr	401	1120	2.93	3.3	538	415	6.05	2.51
Pt PCM	401	1130	2.79	3.2	539	419	6.11	2.66
Pt PCF3	399	1257	2.93	3.7	538	415	8.00	3.31
Pt PCN	401	1245	2.56	3.2	539	413	6.62	2.73
Pt PF5	390	910	2.68	2.4	539	460	22.3	10.3

ergy π,π^* states result from transitions between the two highest occupied molecular orbitals, a_{1u} and a_{2u}, and the lowest unoccupied molecular orbital, a doubly degenerate e_g. These are shown in Fig. 2. The lowest-energy states, B and Q, derive from mixing of the two singly excited configurations $^1(a_{1u}e_g)$ and $^1(a_{2u}e_g)$, both of which have E_u symmetry and have similar energies.

Gouterman [14] derived expressions for the Hamiltonians for the B and Q states in terms of the two singly excited configurations and for the transition moments for the transitions between the ground state and the B and Q states. From these, the relative energies of the frontier molecular orbitals can be obtained. In his treatment of porphyrin spectra, Gouterman defined several quantities: A_{1g} is the mean energy difference between the a_{1u} and the a_{2u} orbitals; A_{1g}' is the energy difference between the e_g orbitals and A_{1g} (Fig. 4); and A_{1g}'' is the configuration interaction between the two one electron excited state configurations. The derivation of these parameters

is given in the Appendix and the results are listed in Table II.

Trends can be seen in the values of A_{1g}, A_{1g}', and A_{1g}'' as a function of phenyl substitution. As the phenyl groups become increasingly electron rich, the gap between the e_g and the HOMO (a_{1u} or a_{2u}), A_{1g}', decreases and the configuration interaction energy decreases. The trend is clearly seen with Pt NH2, Pt POH, Pt TPP, and Pt PF5. The other porphyrins, Pt PBr, Pt PCM, Pt PCF3, and Pt PCN, do not differ statistically from Pt TPP. The same trend can be seen in A_{1g} excluding Pt NH2 (vide infra). Nodes through the meso position of the a_{1u} orbital preclude transmission of resonance or inductive effects from the phenyl substituents. Thus the energy of the a_{1u} orbital is constant through the series of substituted platinum tetraarylporphyrins. A decrease in A_{1g} indicates an increase in the relative energy of the a_{2u} orbital, while a decrease in A_{1g}' indicates a decrease in the relative energies of the e_g orbitals.
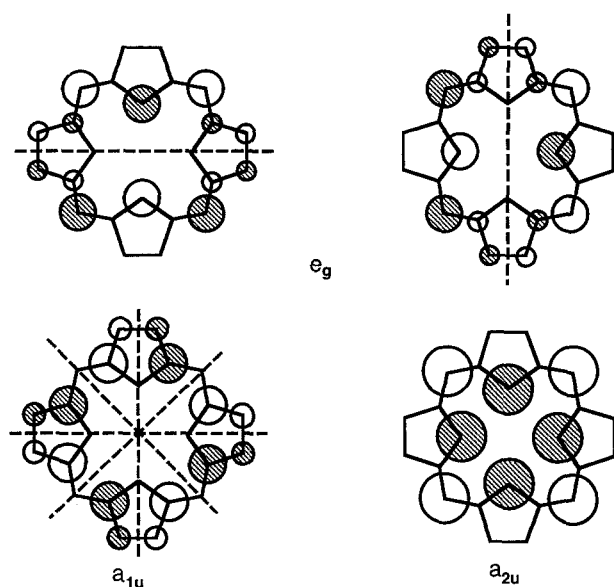
Fig. 2. Frontier molecular orbitals for porphyrin.

The absorption spectra of Zn TPP and Pt TPP were measured in mixtures of THF and N,N-dimethylaniline and neat N,N-dimethylaniline. No changes in the absorption spectra were noted.

Emission Spectra and Lifetimes

The phosphorescence spectrum for Pt TPP in tetrahydrofuran at 25°C is shown in Figure 3. The emission maxima for the substituted platinum porphyrins are listed in Table III. Substitution of electron releasing groups at the *para* position of the platinum tetraphenylporphyrins results in a red shift in the emission maximum, while electron withdrawing groups shift the maximum slightly to the blue. The phosphorescence phase and modulation vs frequency curves for the substituted platinum por-

phyrins were measured in tetrahydrofuran at 25°C. The data were satisfactorily fit to two components, a single exponential decay and scattered excitation light. The measured lifetimes and emission yields for the substituted platinum porphyrins are listed in Table III. The data show a general increase in both the radiative and the nonradiative rate constants upon substitution of Pt TPP at the *para* position; the nonradiative rate constants are affected more than the radiative rate constants. Except for the Pt PF5, the effect of substitution on the radiative and nonradiative rate constants is small.

The emission spectra for several of the porphyrins studied display a band just to the blue of the phosphorescence in tetrahydrofuran at 25°C. This band was assigned to E-type delayed fluorescence. Similar bands in the room temperature emission spectra of Pt etio and Pd TPP have been assigned to E-type delayed fluorescence by Gouterman *et al.* [19]. The maxima of the delayed fluorescence for the substituted porphyrins are listed in Table III. The prompt emission spectrum was recorded in 1-methyltetrahydrofuran at 77 K. No prompt fluorescence or delayed fluorescence was observed; the limit of detection is $\Phi = 1 \times 10^{-5}$. The detection of fluorescence is limited by low levels of metalloporphyrin impurities in the sample. The rate constant for intersystem crossing can be estimated from these data. The radiative rate constant for the excited singlet state can be calculated using the Strickler–Berg equation [18]:

$$k_{rad} = 2.880 \times 10^{-9} n^2 (g_l/g_u)\langle v_f^{-3}\rangle^{-1} \int e(v)d\ln v \quad (1)$$

where n is the refractive index of the solvent, g_l and g_u are the multiplicities of the ground and excited states, respectively, v_f is the fluorescence spectrum in wavenumbers, and v is the absorption energy in wavenumbers. The average fluorescence spectrum was measured from the delayed fluorescence spectrum. The refractive index of THF is 1.41. This and the absorption

Table II. Hammet value, Ratio of Dipole Strengths, Energy Difference Between the B and the Q Bands, and Molecular Orbital Coefficients A_{1g}, A_{1g}', and A_{1g}'' for Substituted Pt *meso*-Tetraarylporphyrins

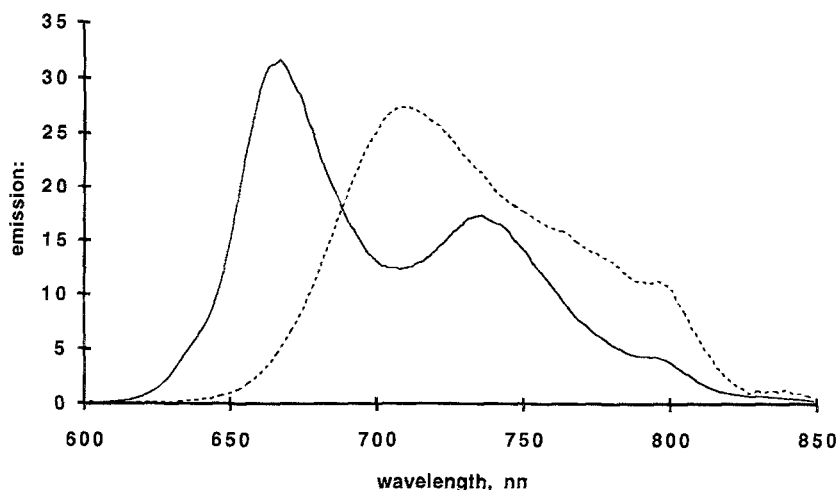|	σ_p^+	q^2_Q/q^2_B	ΔE_{BQ} (cm^{-1})	A_{1g} (cm^{-1})	A_{1g}' (cm^{-1})	A_{1g}'' (cm^{-1})
Pt PNH2	−1.3	0.0108	5823	696±20	21030±80	2912±80
Pt POH	−0.92	0.0052	6104	506	21650	3052
Pt TPP	0	0.0081	6441	671±15	21860±70	3221±70
Pt TBr	0.15	0.0076	6351	643	21780	3176
Pt PCM	0.48	0.0081	6388	668	21760	3194
Pt PCF3	0.612	0.0090	6476	713±17	21850±80	3238±80
Pt PCN	0.659	0.0086	6385	686	21760	3193
Pt PF5	0.49	0.0422	7100	1714	22200	3550

Fig. 3. Emission spectra for Pt TPP (——) and Pt PNH2 (----) in fluid solution.

Table III. Phosphorescence Lifetimes, Phosphorescence Yields, Rate Constants for Nonradiative and Radiative Decay, and Maxima for Phosphorescence and Delayed Fluorescence for Pt *meso*-Tetraarylporphyrins

	τ_p (10^{-6} s)	Φ_p	k_{nrad} (10^4 s^{-1})	k_{rad} (10^3 s^{-1})	P(max) (nm)	DF(max) (nm)
Pt PNH2	20.0±0.1	0.085±0.01	4.6±0.2	4.3±0.4	702	557
Pt POH	39.3±0.2	0.15±0.02	2.2±0.1	3.8±0.4	690	554
Pt POMe					681	
Pt TPP	54.8±0.3	0.19±0.02	1.5±0.1	3.5±0.4	671	555
Pt TBr	46.5±0.2	0.14±0.01	1.8±0.1	3.0±0.3	660	
Pt PCM	34.5±0.2	0.16±0.02	2.4±0.1	4.6±0.5	666	
Pt PCF3	53.5±0.3	0.20±0.02	1.5±0.1	3.7±0.4	661	551
Pt PCN	26.5±0.2	0.12±0.01	3.3±0.2	4.5±0.5	662	
Pt PF5	2.7±0.02	0.019±0.002	36. ±1.8	7.0±0.7	653	

spectrum lead to a radiative lifetime of 66 ns. This value compares well to those calculated for other metalloporphyrins [12]. The prompt fluorescence has a yield of less than 10^{-5}. This leads to a nonradiative decay rate constant from the singlet excited state of greater than 1.5×10^{12} s^{-1}. The estimated excited singlet-state lifetime for platinum tetraphenylporphyrin is then less than 0.7 ps. This is close to the value estimated by Gouterman *et al.* for platinum etioporphyrin [19].

DISCUSSION

The objective of this study was to examine the effect of peripheral substitution on the absorption spectra and excited state properties of porphyrins. Gouterman and co-workers' use of simple MO theory and the fron-

tier molecular orbitals of the porphyrins has provided a useful model for rationalizing absorption spectra. Computational studies have supported the hypothesis that the porphyrin visible absorption bands derive from transitions between the two highest occupied molecular orbitals, a_{1u} and a_{2u}, and the lowest unoccupied molecular orbital, e_g [20]. Unlike the singlet-state transitions, which are mixtures of $^1(a_{1u}e_g)$ and $^1(a_{2u}e_g)$, the transitions between the triplet and the singlet states are pure one-electron configurations [21]. The effect of peripheral substitution on the triplet-state energy can thus be examined in terms of the HOMO and LUMO only. Since the excited singlet and triplet states of the platinum porphyrins are π,π^* in character, the substituent effects on the frontier molecular orbitals should allow one to predict changes in both the visible absorption bands and the phosphorescence bands.

The observed red shift in the phosphorescence with

substitution of increasingly electron-rich substituents must correlate with the decrease in both the energy gap between a_{1u} and a_{2u}, A_{1g}, and that between e_g and the mean energy between a_{1u} and a_{2u}, A_{1g}' (Table II). A previous study has determined that the a_{1u} orbital lies 370 cm^{-1} higher in energy than the a_{2u} orbital for platinum tetraphenylporphyrin [16]. The a_{1u} orbital has nodes at the *meso* positions which prohibit conduction of resonance or inductive effects from the *meso*-aryl substituents to the porphyrin nucleus. For the Pt *meso*-substituted porphyrins, the a_{1u} orbital is constant in energy. It follows that e_g decreases while a_{2u} increases with respect to a_{1u} upon substitution by increasingly electron-rich substituents. The same decrease in e_g with respect to a_{1u} is seen in the red-shifted phosphorescence spectra. If only inductive effects were operative, one would expect both a_{2u} and e_g to be destabilized with such substitution. The opposite substituent effects on e_g and a_{2u} indicate that resonance effects must play a role in the interaction between *meso*-aryl substituents and the porphyrin nucleus [22].

Rotation of the *meso*-phenyl groups into the plane of the porphyrin results in mixing of the phenyl HOMO with the nearby a_{2u} orbital of the porphyrin. The phenyl LUMO stabilizes the e_g orbital. Increasing the electron density of the phenyl groups, e.g., by substitution of *p*-OH, destabilizes the phenyl HOMO and LUMO. The concomitant decrease in the a_{2u}-phenyl(HOMO) energy gap destabilizes the a_{2u} orbital. While the e_g-phenyl(LUMO) energy gap increases leading to a destabilization of the e_g orbital. These trends are illustrated qualitatively in Fig. 4. The lowest steric energy conformation of *meso*-tetraphenylporphyrin has the phenyl groups perpendicular to the porphyrin ring [23]. The increased stabilization through resonance must overcome
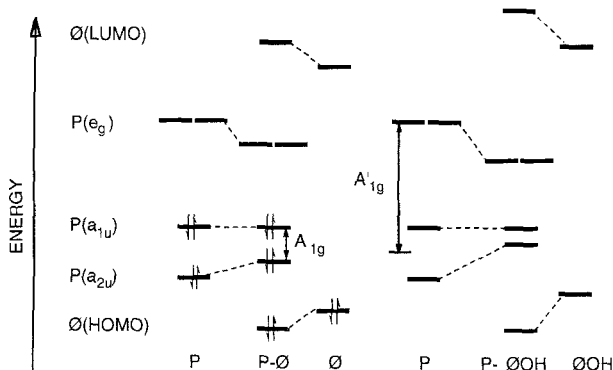
the increase in steric energy with rotation of the phenyl groups. The driving force for resonance interaction between the substituents and the porphyrin ring is the electronegativity of the platinum, which tends to make the porphyrin ring electron poor [24].

The foregoing explanation is consistent with the phosphorescence spectra. The triplet-state configuration is $^3(a_{1u}e_g)$. A plot of triplet-state energy vs σ_p^+ (Fig. 5) shows that electron donating groups lower the triplet-state energy. Since a_{1u} is unaffected by substitution, e_g is stabilized with increasing electron donating substituents. The small value for ρ, 0.03, indicates only a small stabilization of charge on the porphyrin ring. This observation is consistent with the small changes seen in the MO parameters A_{1g} and A_{1g}''.

The Q band intensity and the value for A_{1g} reach a minimum for Pt *p*-hydroxyphenylporphyrin. In the four-orbital model, when a_{1u} and a_{2u} become degenerate, transitions to the first excited state are totally forbidden. As the *meso* substituents become increasingly electron rich, these orbitals become isoenergetic and the Q(0,0) band for the *p*-hydroxy-substituted porphyrin nearly disappears [25]. Further destabilization of a_{2u} results in the Q band regaining intensity. This trend is seen in Table II. A similar trend has been reported by Spellane *et al.* [17], where the energy gap between the HOMO, a_{1u}, and the NHOMO, a_{2u}, decreases from Pd PF5 to Pd TPP.

An alternative explanation has been advanced concerning the behavior of aminophenyl substituted porphyrins [26]. Zinc tetraphenylporphyrins, when substituted at the *ortho* position by amino groups, show changes in the absorption spectra similar to those seen with Pt TPP; the B band broadens, decreases in magnitude, and shifts slightly to the red compared to the tetraphenylporphyrin. The Q bands remained unaffected. The broadening of the B band was ascribed to charge–transfer interactions between the amine and the porphyrin e_g orbital. Two observations make such charge–transfer interactions unlikely. The free energy change for electron transfer for either Zn *meso*-tetra (*o*-aminophenyl)porphyrin or Pt PNH2 is endothermic [27]. Also, no changes in the spectra of either Zn TPP or Pt TPP were seen upon the addition of dimethylaniline at concentrations up to neat liquid. Finally, charge–transfer interactions would not explain the narrowing of the B band seen with Pt PF5. Of note, however, is that similar broadening of the B band was seen in a related ortho-amino-substituted Zn TPP [26] in which the *meso*-phenyl groups were fixed perpendicular to the porphyrin ring. This should preclude any resonance interaction between the *meso* substituents and the porphyrin nucleus.

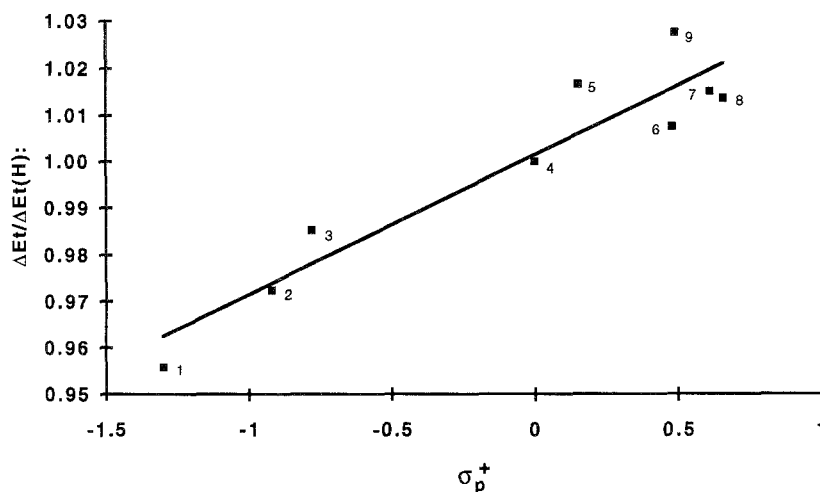As part of this study, the CI energy was determined

Fig. 4. Qualitative molecular orbital diagram for the interaction of the phenyl (Ø) HOMO and LUMO with the porphyrin (P) frontier molecular orbitals for Pt TPP and Pt POH.

Fig. 5. The triplet-state energy for Pt tetraarylporphyrins normalized to Pt TPP vs the Hammett substituent constants σ_p^+, where the substituents are *p*-aminophenyl (1), *p*-hydroxyphenyl (2), *p*-methoxyphenyl (3), phenyl (4), *p*-bromophenyl (5), *p*-carbomethoxyphenyl (6), *p*-cyanophenyl (7), *p*-trifluoromethyl (8), and pentafluorophenyl (9). The Hammett value for 8 was obtained from the sum $(3 \times \sigma_p^+) + (2 \times \sigma_m)$.

for this series of porphyrins. The effect of substitution on the CI energy determined here is at odds with a previous study. In a series of metalloporphyrins, Shellnut and Ortiz [16] found a correlation between the CI matrix element, A_{1g}'', and the electronegativity of the peripheral substituents determined from the sum of the Hammett σ_m values. With the exception of porphine itself, the CI energy was found to decrease with increasing electron withdrawing ability of the substituents [28,29]. Figure 6a, from Ref. 16, is reproduced with the point for Pt PF5, determined in the present study, included. Pt PF5 does not follow the proposed correlation. Since resonance effects have been shown to be important in determining the relative energies of the frontier orbitals, A_{1g}'' was, instead, plotted against σ_p^+, shown in Fig. 6b. The data from Ref. 16 could not be plotted in Fig. 6b because appropriate substituent constants could not be found. Nevertheless, the correlation is clearly in the opposite direction. It should be noted that the point for Pt PF5 should be considered a maximum; the approximation $A_{1g}/A_{1g}'' < < 1$ no longer holds when the two single-electron configurations are far from degeneracy (see Appendix). Increased electron–electron repulsion in the porphyrin ring is expected to increase the CI energy [15]. Electron releasing groups are expected to expand the molecular orbital coefficients, relieving electron–electron repulsion and thus lowering A_{1g}''. This trend is borne out in Fig. 6b. Shelnutt and Ortiz proposed that resonance interaction between the substituents and the ring accounts for a significant portion of the CI energy. However, they

also proposed that the correlation in Fig. 6a results from delocalization of the electrons from the α carbons of the peripheral substituents onto the ring. It is clear from Fig. 6a that this is not so. Instead, the high values for the CI energy for Pt uroporphyrin, Pt octaethylporphyrin, the peripheral substituents of which are electron releasing in character, Pt porphyrin, which has no substituents, and Pt PF5, the substituents of which are electron withdrawing, can all be explained by the lack of resonance interaction of the substituents with the porphyrin frontier molecular orbitals. The carbon P_z orbitals for aliphatic *meso* substituents are too far in energy from the e_g and a_{2u} orbitals to mix substantially with the frontier molecular orbitals of porphyrin. With no substantive resonance interaction between the ring and the substituents, the values for the CI energy for porphyrin, uroporphyrin, octaethylporphyrin, and pentafluorophenylporphyrin are all similar in magnitude: $A_{1g}'' = 3569 \pm 23$ cm^{-1}. On the other hand, the π orbitals of the vinyl groups for protoporphyrin mix with the porphyrin molecular orbitals, and the CI energy is lowered. The trend continues with Pt TPP and is further lowered by electron-rich phenyl substituents.

The phosphorescence yields and lifetimes were determined for the porphyrin series. The large magnitude of both decay rate constants ($k_p \approx 10^3$ s^{-1}, $k_d \approx 10^4$–10^5 s^{-1}) is due to enhanced spin-orbit coupling for platinum arising from mixing of the platinum d_π orbitals and the porphyrin e_g (π*) orbitals [30]. The size of the substituent effects on the nonradiative rate constant is sim-
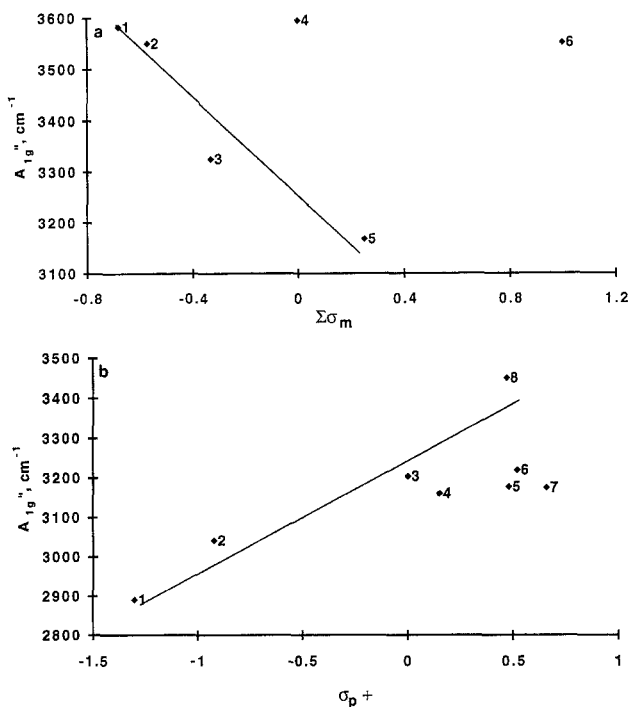
Fig. 6. (a) Configuration interaction matrix element (A_{1g}'') vs the sum of the Hammett substituent constants σ_m for uroporphyrin (1), octaethylporphyrin (2), protoporphyrin IX (3), porphine (4), tetraphenylporphyrin (5), and meso-tetra(pentafluorophenyl)porphyrin (6). Porphyrins 1–4 are from Ref. 16; porphyrins 5 and 6 are from this work. (b) Configuration interaction matrix element (A_{1g}'') vs the sum of the Hammett substituent constants σ_p^+ for the Pt arylporphyrins where the substituents are p-aminophenyl (1), p-hydroxyphenyl (2), phenyl (3), p-bromophenyl (4), p-carbomethoxyphenyl (5), p-cyanophenyl (6), p-trifluoromethyl (7), and pentafluorophenyl (8). The Hammett value for 8 was obtained from the sum $(\sigma_p^+ \times 3) + (\sigma_m^+ \times 2)$.

ilar to those seen by Harriman and Hosie in a study of the substituent effects on the excited singlet-state properties of substituted tetraphenylporphyrins [13]. In this study, only the rate constants for Pt PF5 differ significantly from Pt TPP; the radiative rate constant is greater by about a factor or two and the nonradiative rate constant is greater by over an order of magnitude. Interestingly, the sum of the Hammett values for the five fluorines makes pentafluorophenyl only moderately electron withdrawing, $\sigma_p^+ = 0.49$; cyanophenyl is more electron withdrawing, $\sigma_p^+ = 0.66$. Harriman and Hosie found no similar effect for either a para-cyano or a para-nitro, $\sigma_p^+ = 0.79$, substituent. It could be argued that the ortho-fluorine substituents keep the phenyl ring perpendicular to the porphyrin ring. However, fluorine substituents are quite small [31]; molecular models indicate little steric interaction between the ortho-fluorine and the

pyrrole hydrogen. Moreover, with the model presented above, little energy is to be gained upon rotation of the perfluorophenyl ring into the plane of the porphyrin. More likely, the degree of electron withdrawing ability of the pentafluorophenyl substituent is not adequately expressed by the sum of σ_m and σ_p^+.

Interaction between the porphyrin e_g orbital and the Pt d_π orbital is thought to lead to enhanced spin-orbit coupling [24]. The metal d_π orbitals are lower in energy than the porphyrin frontier molecular orbitals. A destabilization of e_g with substitution of electron withdrawing groups as seen in the phosphorescence spectra should lessen the d_π–e_g mixing and lower the k_{rad} and k_{nrad}. On the other hand, an increase in k_{rad} and k_{nrad} over the series Pd TPP, Pt TPP, Pt PF5 correlates to the increase in e_g energy also seen. The a_{1u} orbital is constant in energy upon metal substitution under d_{4h} symmetry due to nodes at the pyrrole nitrogens. The e_g orbital is destabilized on replacement of Pd by Pt in porphyrins [24]. Since little change is expected in the d_π orbital itself with changes between Pd and Pt, factors in addition to d_π–e_g interaction may be responsible for enhanced intersystem crossing.

CONCLUSION

Pt porphyrins substituted at the meso position by substituents with electron-rich orbitals capable of interacting with the porphyrin π orbitals cause a red shift in both the absorption and the phosphorescence spectra. Conventional green light-emitting diodes have a maximum emission between 555 and 570 nm. The peak sensitivity of a silicon-based detector is at 800 nm. Stabilizing the Pt porphyrin nucleus with electron-rich substituents at the meso positions leads to better overlap with this combination of excitation source and detector. One would expect, for example, Pt tetra (p-N,N-dimethylanilino)porphyrin to be a better choice under these conditions. Qualitatively, the substituent effects should be similar Pd porphyrins. A small destabilization of the a_{2u} orbital and a larger stabilization of the e_g orbital lead to red shifts in both the absorption and the phosphorescence spectra compared to Pt porphyrins. A further prediction is that Pt tetraphenylporphyrins substituted with strongly electron donating groups should have phenyl groups which are more coplanar with the porphyrin ring. Molecular modeling is being used to determine the trade-off between resonance stabilization and steric hindrance.

The efficiency of quenching of phosphorescence by oxygen is given by the Stern–Volmer relation and is a function of the diffusivity of oxygen through the medium

containing the porphyrin and the phosphorescent lifetime of the porphyrin. The longer triple-state lifetimes of Pd porphyrins make them more suitable for measuring low concentrations of oxygen than Pt porphyrins. Alternatively, a polymer with a higher oxygen diffusivity can be used with the Pt porphyrins, yielding faster responses to oxygen. These aspects of porphyrins as oxygen sensors are the basis of a future publication.

APPENDIX

Gouterman [15] derived expressions for the Hamiltonians for the B and Q states in terms of the two singly excited configurations and for the transition moments for the electronic transitions between the ground state and the B and Q states. From these, the relative energies of the frontier molecular orbitals can be obtained. From Gouterman, the quantity A_{1g} represents the splitting in energy of the a_{1u} and a_{2u} orbitals, A_{1g}' is the energy difference between the e_g orbitals and A_{1g}, and A_{1g}'' represents the configuration interaction (CI) energy between the two one-electron configurations. The energies of the B and Q states are obtained from rigorous solution of the 2×2 matrix generated from mixing of the two configurations and are given by

$$E_B = A_{1g}' + A_{1g}''/\cos(2v) \tag{2}$$

$$E_Q = A_{1g}' - A_{1g}''/\cos(2v) \tag{3}$$

where $\tan(2v) = A_{1g}/A_{1g}''$.

In the case of platinum tetraphenylporphyrins, the a_{1u} and a_{2u} orbitals are nearly degenerate [15] and the configuration interaction is high. In such circumstances A_{1g}/A_{1g}'' is expected to be small and certain assumptions can be made. As v approaches zero, $\cos(2v)$ approaches unity and

$$E_B = A_{1g}' + A_{1g}'' \tag{4}$$

$$E_Q = A_{1g}' - A_{1g}'' \tag{5}$$

This is the special case where the B and Q states are made up of nearly 50/50 mixtures of the two single-electron configurations. The excited states made up equally of the singly excited configurations are defined by Gouterman as reference states, B° and Q°. If the transition moments for the two configurations are similar, $R(a_{1u}, e_g) \approx R(a_{2u}, e_g)$, then transitions from the ground to the Q state are totally forbidden and those to the B state totally allowed [15].

The changes in the absorption spectra of platinum tetraarylporphyrins produced by substitution on the phenyl

groups can be thought of as small perturbations on B° and Q°. Gouterman [15] obtained an expression for the transition moment of the Q state by setting $r = 0$ and using second-order perturbation theory. For tetraphenylporphyrins (32) the expression becomes

$$(R_Q)^2 = [A_{1g}/(E_Q - E_B)]^2 R_B^2 \tag{6}$$

In terms of the observed quantities, the expression is

$$\epsilon_q = 2[A_{1g}]^2[2500(R_B)^2/(E_Q - E_B)^2](\Delta v/v) \tag{7}$$

where ϵ_q is the molar extinction coefficient of the Q(0,0) band, E_Q and E_B are the energies of the Q and B bands, and Δv is the width at half-maximum for the Q band. Using the assumptions of near-degeneracy of the $^1(a_{2u}e_g)$ and $^1(a_{1u}e_g)$ configurations, three of the four MO parameters can be determined, A_{1g}, A_{1g}', and A_{1g}''.

ACKNOWLEDGMENTS

REFERENCES

1. W. L. Rumsey, J. M. Vanderkooi, and D. F. Wilson (1988) *Science* **241**, 1649.
2. M. Vanderkooi, G. Maniara, T. J. Green, and D. F. Wilson (1987) *J. Biol. Chem.* **262**, 5476.
3. J. M. Vanderkooi, W. W. Wright, and M. Erecinska (1990) *Biochemistry* **29**, 5332.
4. D. B. Papkovsky, J. Olah, I. V. Troyanovsky, N. A. Sadovsky, V. D. Rumyantseva, A. F. Mironov, A. I. Yaropolov, and M. P. Savitsky (1992) *Biosens. Bioelectron.* **7**, 199.
5. J. Kavandi, J. Callis, A. Gouterman, G. Khalil, D. Wright, E. Green, D. Burns, and B. McLachlan (1990) *Rev. Sci. Instrum.* **61**, 3340–3347.
6. A. Sharma and O. S. Wolfbeis (1988) *Appl. Spectrosc.* **42**, 1009.
7. N. Opitz and D. W. Lübbers (1987) *Int. Anesthesiol. Clin.* **25**, 177.
8. The partial pressure of oxygen in human arterial blood can vary from 40 to 680 mm Hg.
9. A. D. Adler, F. R. Longo, J. D. Finarelli, J. Goldmacher, J. Assour, and L. Korsakoff (1967) *J. Org. Chem.* **32**, 476.
10. J. S. Lindsey, I. C. Schreiman, H. C. Hsu, P. C. Kearney, and A. M. Marguerettaz (1987). *J. Org. Chem.* **52**, 827.
11. A. D. Adler, D. Eastwood, and M. Gouterman (1970) *J. Mol. Spectrosc.* **35**, 359.
12. P. G. Seybold and M. Gouterman (1969) *J. Mol. Spectrosc.* **31**, 1.
13. A. Harriman and J. R. Hosie (1981) *J. Chem. Soc. Faraday Trans.* **77**, 1695.
14. M. Gouterman (1978) in D. Dolphin (Ed.), *The Porphyrins*, Academic Press, New York, Vol. 3, p. 12.
15. M. Gouterman (1959) *J. Chem. Phys.* **30**, 139.
16. J. A. Shelnutt and V. Ortiz (1985) *J. Phys. Chem.* **89**, 4733.
17. P. J. Spellane, M. Gouterman, A. Antipas, S. Kim, and Y. C. Lin (1980) *Inorg. Chem.* **19**, 386.
18. S. J. Strickler and R. A. Berg (1962) *J. Chem. Phys.* **37**, 814.

19. J. B. Callas, M. Y. Gouterman, M. Jones, and B. H. Henderson (1971) *J. Mol. Spectrosc.* **39**, 410.

20. C. Weiss, H. Kobayashi, and M. Gouterman (1965) *J. Mol. Spectrosc.* **16**, 415.

21. M. Gouterman (1978) in D. Dolphin (Ed.), *The Porphyrins*, Academic Press, New York, Vol. 3, p. 95.

22. The same conclusion was reached by Shelnutt and Ortiz. In Ref. 15 both A_{1g} and A_{1g}' decrease on going from Pt porphyrin to Pt tetraphenylporphyrin even though phenyl groups are electron withdrawing groups, $\sigma_m = 0.05$.

23. S. J. Chantrell, C. A. McAuliffe, R. W. Munn, A. C. Pratt, and R. F. Weaver (1977) *Bioinorg. Chem.* **7**, 283.

24. J. A. Shelnutt (1984) *J. Phys. Chem.* **88**, 4988.

25. The values for A_{1g} in Table II for Pt POH and Pt PNH2 should be considered a maximum since it was difficult to resolve the $Q(0,0)$ band from the tail of the Q(1,0) band.

26. J. S. Lindsey, J. K. Delanay, D. C. Mauzerall, and H. Linschitz (1988) *J. Am. Chem. Soc.* **110**, 3610.

27. The singlet-state energies for Zn *meso*-tetra(*o*-aminophenyl)porphyrin or Pt PNH2 are 2.09 and 2.25 eV, respectively. The reduction potentials for Zn TPP and Pt TPP are -1.35 and -1.46 V vs SCE [from R. H. Felton (1978) in D. Dolphin (Ed.), *The Porphyrins*, Academic Press, New York, Vol. 5]. The oxidation potential of aniline is 0.88 V vs SCE [from L. Meites, P. Zuman, and E. Rupp (Eds.) *CRC Handbook Series in Organic Electrochemistry*, CRC Press, Boca Raton, FL, 1982, Vol. 5]. This yields, neglecting the coulombic term, $\Delta G_{et} = 0.14$ eV for Zn TPP and $\Delta G_{et} = 0.09$ eV for Pt TPP.

28. Acetate and propionate for uroporphyrin, ethyl for octaethylporphyrin, phenyl for tetraphenylporphyrin, and vinyl, methyl, and propionate for protoporphyrin. No correlation was found for porphine.

29. The Hammet substituent values were obtained from the following sources: (a) R. W. Alder, R. Baker, and J. M. Brown (1972) *Mechanism in Organic Chemistry*, Wiley Interscience, New York; (b) O. Exner (1976) in N. B. Chapman and J. Shorter (Eds.), *Correlation Analysis in Chemistry: Recent Advances*, Plenum Press, New York; (c) J. March (1977) *Advanced Organic Chemistry*, McGraw-Hill, New York; (d) P. N. Craig (1971) *J. Med. Chem.* **14**, 680.

30. M. Gouterman (1978) in D. Dolphin (Ed.), *The Porphyrins*, Academic Press, New York, Vol. 3. This mixing also destabilizes the e_g orbitals, resulting in a blue shift of the B band. This shift is more pronounced as the metal is changed from row 2 to row 3 in the periodic table, for example, Pd to Pt.

31. The van der Waals volume for fluorine is 87% larger than an aromatic hydrogen and 56% the size of an amino group: J. T. Edward (1970) *J. Chem. Ed.* **47**, 261. A separate calculation for molecular volumes has an aromatic fluorine only slightly larger than an aromatic hydrogen: 15.11 to 14.90 [O. Exner (1967) *Collect. Czech. Chem. Commun.* **32**, 1]. Molar refractivities, used in structure-activity relationships, actually have fluorine smaller than hydrogen: 25.36 for C_6H_5 and 23.98 for C_6F_5 [C. Hansch, A. Leo, S. H. Unger, K. H. Kim, D. Nikaitani, and E. J. Lien (1973) *J. Med. Chem.* **16**, 1207].

32. Only the elements of A_{1g} symmetry mix the B and Q states for Pt tetraarylporphyrins.